RESEARCH ARTICLE

Open Access

CrossMark

Hydrous Na-garnet from Garnet Ridge; products of mantle metasomatism underneath the Colorado Plateau

Kunihiko Sakamaki[*], Yuto Sato and Yoshihide Ogasawara

Abstract

This is the first report on amphibole exsolution in pyrope from the Colorado Plateau. Pyrope crystals delivered from mantle depths underneath the Colorado Plateau by kimberlitic volcanism at 30 Ma were collected at Garnet Ridge, northern Arizona. The garnet grains analyzed in this study occur as discrete crystals (without adjacent rock matrix) and are classified into two major groups, Cr-rich pyrope and Cr-poor pyrope. The Cr-poor pyrope group is divided into four subgroups based on exsolved phases: amphibole lamella type, ilmenite lamella type, dense lamellae type, and clinopyroxene/amphibole lamellae type. Exsolved amphibole occurs in amphibole lamella type, dense lamellae type, and clinopyroxene/amphibole lamellae type of Cr-poor pyrope. The amphibole crystals tend to have preferred orientations in their garnet hosts and occur as monomineralic hexagonal or rhombic prisms and tablets, and as multimineralic needles or blades with other exsolved phases. Exsolved amphibole has pargasitic compositions (Na_2O up to 1.6 apfu based on 23 oxygen). Garnet host crystals that have undergone amphibole exsolution have low OH contents (2–42 ppmw H_2O) compared to garnets that do not have amphibole lamellae (up to 115 ppmw H_2O). The low OH contents of garnets hosting amphibole lamellae suggest loss of OH from garnet during amphibole exsolution. Amphibole exsolution from pyrope resulted from breakdown of a precursor "hydrous Na-garnet" composition $(Mg,Na_x^+)_3(Al_{2-x}, Mg_x)_2Si_3O_{12-2x}(OH)_{2x}$. Exsolution of amphibole and other phases probably occurred during exhumation to depths shallower than 100 km prior to volcanic eruption.

Based on the abundance and composition of exsolved clinopyroxene and amphibole lamellae in one garnet, hydrous Na-garnet had excess silicon ($Si_{3.017}$ apfu, 12 oxygen normalization, vs. $X_3Y_2Si_3O_{12}$ for typical garnet). Comparison with experimental data suggests crystallization at pressures near 6–8 GPa. Garnet crystals that host exsolved amphibole have compositions (Pyp_{49-76}, 3–10 wt% CaO, and up to 0.6 wt% Cr_2O_3) similar to garnets reported from pyroxenites, and have pyrope-almandine-grossular compositional ranges that overlap with the Cr-rich pyrope (typical lherzolitic garnet).

Hydrous Na-garnet was likely formed by metasomatic reactions between Cr-rich pyrope and Na-rich aqueous fluid in the deep upper mantle. The most likely source of metasomatic Na-rich fluid is ancient oceanic crust that was subducted before subduction of the Farallon Plate beneath the Colorado Plateau.

Keywords: Hydrous Na-garnet, The Colorado Plateau, Amphibole exsolution, Pyrope, Mantle metasomatism

* Correspondence: k.sakamaki@akane.waseda.jp
Department of Earth Sciences, Waseda University, 1-6-1 Nishiwaseda,
Shinjuku-ku, Tokyo 169-8050, Japan

Springer Open

Sakamaki *et al. Progress in Earth and Planetary Science* (2016) 3:20

Page 2 of 17

Background

Various garnet crystals and garnet-bearing xenoliths occur at Garnet Ridge, northern Arizona, USA (Switzer 1975). These garnets were delivered to the surface from a wide range of depths from the deep mantle to crustal levels underneath the Colorado Plateau by a kimberlitic diatreme associated with the Navajo volcanic field during Oligocene time (e.g., Watson and Morton 1969). The kimberlitic diatreme at Garnet Ridge has been studied by many researchers (e.g., Gregory 1916; Switzer 1975; Wang et al. 1999; Smith et al. 2004), in part, because pyrope crystals carried by the diatreme have origins of great depths from the upper mantle. These pyrope crystals have wide chemical variations and various inclusions/exsolved phases such as silicates, sulfides, oxides, titanates, fluid/melt, and composite grains of these phases (e.g., Wang et al. 1999, 2000; Sato and Ogasawara 2013, Sato et al. 2014). The variations of chemistry, inclusion phases, and exsolved phases suggest heterogeneities in the shallow to deep mantle underneath the Colorado Plateau.

We discovered exsolved amphibole in some of pyrope crystals from Garnet Ridge; this paper is the first report on exsolution lamellae of Na-bearing amphibole in pyrope from the Colorado Plateau. Exsolution of Na-bearing amphibole from pyrope indicates that Na and OH components were enriched in garnet prior to exsolution (Song et al. 2005). At present, reports on Na-rich (>1 wt% Na_2O) garnet are limited to inclusions in diamond from kimberlite pipes in South Africa and other localities (e.g., Moore and Gurney 1985; Sautter et al. 1991). Significant amounts of Na in garnet are evidence of ultrahigh pressure (UHP) conditions (Sobolev and Lavrent'ev. 1971; Bishop et al. 1978). Except for hydrogrossular-andradite, garnet that forms at low pressure is a nominally anhydrous mineral, but OH has been identified in garnet of mantle origin at concentrations ranging up to hundreds of ppmw (ppm wt% as H_2O) (Aines and Rossman 1984; Ogasawara et al. 2012, 2013). Significant amounts of OH in pyrope-rich garnet are regarded as evidence of H_2O-rich environments at UHP conditions (Withers et al. 1998; Mookherjee and Karato 2010). In this study, we describe pyrope garnet with exsolution lamellae of Na-rich amphibole, indicating formation from a precursor Na and OH-bearing garnet, namely hydrous Na-rich garnet. We argue that the hydrous Na-rich garnet formed by interactions between mantle peridotite and fluid originating from ancient subducted oceanic crust underneath the Colorado Plateau, and that exsolution of amphibole occurred by decompression during transit to the surface.

Methods

Experimental samples from Garnet Ridge

Garnet Ridge is a northeast-southwest trending ridge composed of the Jurassic Summerville Formation and Bluff sandstone in northern Arizona in the central part of the Navajo volcanic field (Switzer 1975). The Navajo volcanic field is characterized by mid-Tertiary volcanic necks, dikes, lavas, and various intrusions of alkali-rich mafic and ultramafic rocks (Roden et al. 1979; Semken 2003). A xenolith-rich kimberlitic diatreme associated with the Navajo volcanisms erupted through Garnet Ridge at ca. 30 Ma (Smith et al. 2004). Discrete garnet crystals (without surrounding rock matrix), garnet megacrysts, garnet aggregates, and garnet-bearing xenoliths (e.g., lawsonite-eclogite) are scattered on the ridge and the ground of the Carmel Formation and the Entrada sandstone surrounding Garnet Ridge (Watson and Morton 1969; Helmstaedt and Schulze 1988; Usui et al. 2003, 2006, 2007). This study is based on analyses of the discrete garnet crystals.

Analytical methods

Fine-grained inclusion phases were identified by spot analyses and 2D mapping with a laser Raman spectrometer, Horiba Jobin Yvon LabRAM300, at room temperature using a 514.5-nm Ar-ion laser and a 488-nm solid state laser as excitation lines. Unpolarized Raman signals were collected with an MPlan ×100 microscope objective lens (Olympus Co., Tokyo, Japan) with 10 mW power for the Ar-ion laser and 25 mW power for the solid state laser and spot size of ca. 1 μm. The analytical resolution of the Raman spectra is accurate to ±<1 cm^{-1} wavenumbers as calibrated using a Si crystal as a standard.

Elemental compositions and 2D distributions of compositions in host garnet and guest phases were analyzed using an electron microprobe, JXA-8900 (JEOL Ltd., Tokyo, Japan), by electron microprobe wavelength dispersive spectroscopy (EMP-WDS) at Waseda University. Quantitative analyses were conducted using a LaB$_6$ filament under the following conditions: accelerating voltage, 15 or 20 kV; beam current, 20 nA; and and beam diameter, 10 μm. For 2D elemental X-ray mapping, an accelerating voltage of 15 kV, a beam current of 200 nA, and a beam diameter of 1 μm were used.

Water contents in garnet crystals were determined using a micro-Fourier transform infrared (micro-FTIR) spectrometer (Thermo Nicolet, Avatar 370 with Continuum) at Waseda University. In order to obtain high-quality transmission IR spectra, the garnet samples were prepared as double-side polished sections (thickness: ca. 250–500 μm). Measurements were conducted with an aperture size of 100×100 μm and a spectral resolution of 8 cm^{-1} using unpolarized light. Each spectrum was accumulated from 200 iterations on the same spot and was calibrated using polystyrene film as a standard. Peak fitting of IR spectra was conducted by the curve fitting method of the Lorentzian-Gaussian function in order to determine values of peak position, intensity, and full

Sakamaki *et al. Progress in Earth and Planetary Science* (2016) 3:20

Page 3 of 17

width at half maximum (FWHM) were determined for IR absorption bands caused by OH using the LabSpec 4.10 software associated with the Raman spectrometer. We estimate OH concentrations in host garnet using the Beer-Lambert law:

$$C = 18,000 \times I/d/\varepsilon/\rho,$$

where C = water concentration (OH as H_2O, ppmw.), I = integrated IR absorption intensity, d = sample thickness (cm), ε = IR absorption coefficient (L/mol/cm^2) of water (OH) in garnet, and ρ = density of garnet. The absorption intensity I is the integrated intensity of an IR absorption band caused by OH in garnet in the wavenumber range of 3400–3700 cm^{-1}. We used an IR absorption coefficient of 8770 L/mol/cm^2 presented by Katayama et al. (2006) and a density of pyrope of 3.58 g/cm^3 after Deer et al. (1992). Using the uncertainty in I of 510 L/mol/cm^2 reported by Katayama et al. (2006) and estimates of errors in sample thickness, peak fitting, and sample density, we use Gaussian error propagation to calculate relative uncertainties (1σ) in OH contents ranging from 8 % for good conditions (water-rich, thick sample, well-defined baseline) to 14 % for poor conditions (water-poor, thin sample, poorly defined baseline).

A key problem in this study is distinguishing phases that exsolved from garnet versus phases that were overgrown and trapped by garnet (trapped inclusions). We combined microscopic observations, phase mapping by laser Raman spectroscopy, and element mapping by EMP-WDS and used the following criteria to identify exsolved phases: (1) preferred orientation of guest grains indicating a crystallographic relationship between guest grains and host garnet; (2) presence of guest grains in several garnet host crystals of the same type (see below); (3) homogeneous distributions of guest grains in certain areas of garnet host; (4) elemental depletion halos in host garnet around grains (e.g., Ti-poor halo in garnet around Ti-bearing amphibole grain); and (5) a high number of guest grains occurring within garnet host. We regarded inclusion phases satisfying at least three among these five conditions as exsolved phases (i.e., not trapped inclusions) in the strict sense.

Results

Pyrope crystals from Garnet Ridge

Pyrope crystals and their fragments occur as grains approximately 5–25 mm across with red, reddish-brown, purplish, and black colors. We classified pyrope crystals into two major groups (A and B) on the basis of major element chemical compositions: group A is Cr-rich with a limited range of pyrope-content and group B is Cr-poor with more variable pyrope-contents (Table 1).

Group A: Cr-rich pyrope

Cr-rich pyrope looks reddish or purplish-colored by the naked eye (Fig. 1). Individual grains are chemically homogeneous based on microprobe analyses. From grain to grain, chemical compositions show the following ranges: Prp 67–74, Alm 13–18, and Grs 7–11 mol%

Table 1 Classification of garnet on the basis of chemistry and inclusion/lamella phases

Garnet group	Color	Chemistry				Exsolution lamella phases								
		Prp (mol%)	Alm (mol%)	Grs (mol%)	Cr2O3 (wt.%)	Cpx	Amp	Ap	Rt	Ilm	Ctn	Sri	Crm	Cr-Spl
A. Cr-rich pyrope	Red-purple	67–74	13–18	7–11	1.0–6.4				+	+	+	+	+	+
B. Cr-poor pyrope														
B₁. Amp type	Brown	49–66	18–28	16–26	<0.4		++	+	++	++	+	+		
B₂. Ilm-only type	R-brown	49–68	20–38	12–19	0.4–2.0					++				+
B₃. Dense lamellae type	Black	54–72	18–33	12–15	<1.0	++	++	+	++	++		+		
B₄. Cpx-Amp type	Light brown	61–76	13–27	6–11	<0.6	++	+		++	++				

Garnet group	Ol	Opx	Cpx	Ti-Chu	Chl	Spl	Crn	Dol	Mgs	Ap	sulfides	Multi
						Inclusions without lamella textures						
A. Cr-rich pyrope	++	++	++	+	+	+					+	+[a]
B. Cr-poor pyrope												
B₁. Amp type			++		+			+	+	+	+	
B₂. Ilm-only type	++	++	++		+					+	+	++[b]
B₃. Dense lamellae type			++			+	+			+	+	++[c]
B₄. Cpx-Amp type	+	+									+	

Ap apatite, *Ctn* crichtonite, *Sri* srilankite, *Crn* carmichaelite, *Cr-Spl* chromian spinel, *Ti-Chu* titanian clinohumite, *Crn* corundum, *Dol* dolomite, *Mgs* magnesite
[a]Multi phase inclusions composed of Dol, Mgs, Amp, Phl, Rt, Ap, Cr-Spl, and sulfides
[b]Multi phase inclusion composed of gas, liquid-H_2O, and solid phases (rutile, chlorite, calcite, and barite)
[c]Multi phase inclusion composed of Dol, Mgs, Amp, Cpx, Opx, Ab, Ap, Rt, Ilm, and sulfides
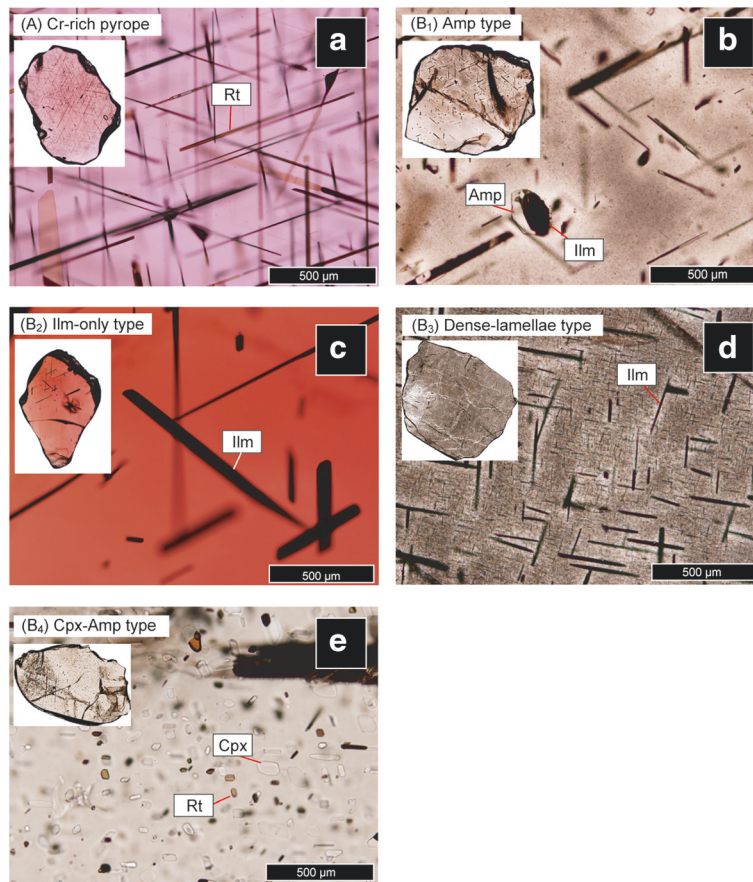
Sakamaki *et al. Progress in Earth and Planetary Science* (2016) 3:20

Page 4 of 17

Fig. 1 Photomicrographs of group A, Cr-rich pyrope garnet and four subgroups of group B, Cr-poor pyrope. **a** Group A: Cr-rich pyrope. **b** B_1: amphibole lamella type. **c** B_2: ilmenite lamella type. **d** B_3: dense lamellae type. **e** B_4: clinopyroxene and amphibole lamellae type

(Fig. 2). The concentrations of Cr_2O_3 range from 1.0 up to 6.4 wt%. The purplish color of group A garnet becomes darker with increasing Cr_2O_3. This garnet contains exsolution lamellae of anhydrous minerals such as rutile, ilmenite, crichtonite [(Sr, Ca, K, Na) (Cr, Fe^{2+}, Fe^{3+}, Ti, V^{3+}, Zr, $Mg)_{21}$(O,OH)$_{38}$], carmichaelite, [(Ti,Cr,-Fe)O_{2-x}(OH)$_x$], and Cr-spinel (Fig. 1 and Table 1). Inclusions of olivine, clinopyroxene, and orthopyroxene were recognized (Table 1). Spherical multiphase inclusions of dolomite, magnesite, amphibole, phlogopite, rutile, apatite, and Cr-spinel are also present.

Group B: Cr-poor pyrope

Group B pyrope crystals are Cr-poor (<2 wt% Cr_2O_3) and show chemical variations in pyrope (49–76 mol%), almandine (13–38 mol%), and grossular (6–26 mol%) components (Figs. 1 and 2). Some group B garnets have Mg-Fe-Ca contents that overlap with group A garnet, but group B shows a wider chemical range to more Ca- and/or Fe-rich compositions (Fig. 2).

The garnets of group B are subdivided into four subgroups based primarily on the identities and abundances of exsolved phases (Tables 1 and 2; Fig. 1). All of the subgroups contain exsolution lamellae of ilmenite, but other exsolved phases vary. Exsolved phases, along with host garnet chemical compositions and colors of the subgroups are described below.

Subgroup B_1, amphibole lamella type (Prp 49–66; Alm 18–28; Grs 16–26 mol%), occurs as reddish-brown-colored pyrope crystals. Subgroup B_1 contains exsolved lamellae of amphibole, rutile, ilmenite, and minor mounts of srilankite [(Ti, Zr)O_2], apatite, and crichtonite. These exsolved phases occur as needles (up to 1 mm in long dimension) consisting of multiple minerals ranging from 20 to 300 μm in length throughout each garnet host crystal. Coarse-grained exsolved minerals are typically surrounded by depletion halos of several to tens of micrometers in width, where fine-grained exsolved phases are absent (Fig. 1). A few chlorite inclusions were identified; they are a primary mineral of hydrated mantle and were trapped during growth of host garnet crystals.

Subgroup B_2, ilmenite lamella only type (Prp 49–68; Alm 20–38; Grs 12–19 mol%; Cr_2O_3 0.4–2.5 wt%), shows red to reddish-brown color and contains exsolved

Sakamaki *et al. Progress in Earth and Planetary Science* (2016) 3:20
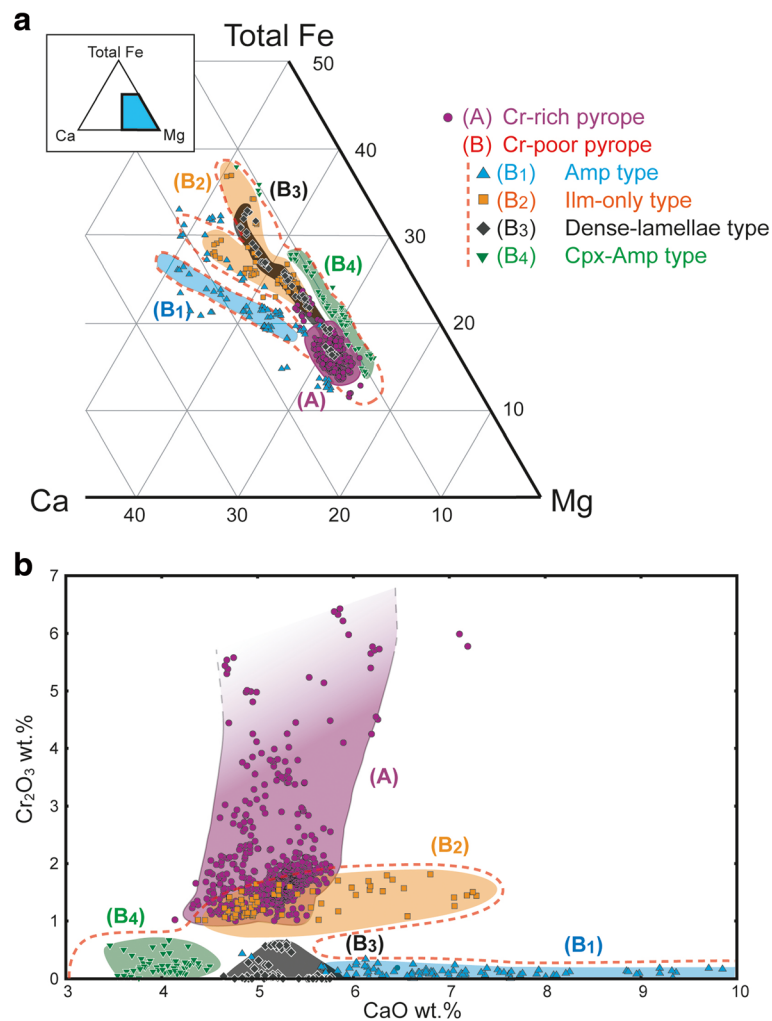
Page 5 of 17

Fig. 2 Compositions of group A and subgroups B₁, B₂, B₃, and B₄ pyrope from Garnet Ridge. **a** Ca-Mg-Fe triangle showing grossular-pyrope-almandine components. **b** CaO vs Cr₂O₃ (wt%). The four subgroups in group B: Cr-poor are characterized by low-Cr₂O₃ contents and varied CaO contents

lamellae of ilmenite only (Fig. 1 and Table 1); no other exsolved phases are recognized. Olivine, orthopyroxene, and clinopyroxene inclusions occur in B_2 pyrope hosts. Composite fluid inclusions consisting of gas, liquid (H_2O), and solid phases (rutile, chlorite, calcite, and barite) are observed in some B_2 garnet grains.

Subgroup B_3, dense lamellae type (Prp 54–72; Alm 18–33; Grs 12–15 mol%), appear very dark due to abundant, densely packed exsolution lamellae of rutile, amphibole, and ilmenite with minor amounts of clinopyroxene, apatite, and srilankite (Fig. 1 and Table 1). Carbonate (magnesite and dolomite) inclusions arranged along curved planes are sometimes identified. Exsolved clinopyroxene crystals occur as long needles (approx. 300 × 10 μm), short needles (50 × 10 μm), coarse-grained columns (75 × 50 μm), and fine-grained columns (25 × 20 μm) together with rutile, ilmenite, srilankite, apatite,

and amphibole. These various occurrences of exsolved clinopyroxene occur within single grains of B_3 pyrope. Clinopyroxene exsolution from garnet is regarded as evidence of supersilicic (majoritic) compositions of precursor garnet at UHP conditions (Moore and Gurney 1985). Some exsolved clinopyroxene needles and columns are sufficiently coarse-grained (>10 μm across) for quantitative analysis by EPMA, and all of the analyzed grains have Na-bearing diopside or omphacite compositions (Di 68–77 mol%; Na_2O 2.4–4.7 wt%). Exsolved clinopyroxene lamellae in a single host garnet grain have homogeneous compositions, but lamellae in different garnet host crystals may have different compositions. Such grain by grain variations of exsolved clinopyroxene compositions probably reflect differenced in Mg, Fe, and Na contents and excess Si of precursor host garnet prior to exsolution.

Sakamaki *et al. Progress in Earth and Planetary Science* (2016) 3:20

Page 6 of 17

Table 2 Representative chemical compositions of pyrope from Garnet Ridge

	(A) Cr-rich pyrope	(B) Cr-poor pyrope			
		B_1	B_2	B_3	B_4
Wt.%		Amp	Ilm-only	Dense lamellae	Cpx-Amp
SiO_2	41.91	42.24	41.02	41.32	40.40
TiO_2	0.09	0.05	0.14	0.10	0.06
Al_2O_3	22.30	23.36	21.66	23.01	22.72
Cr_2O_3	1.71	0.13	1.46	0.01	0.04
FeO^a	8.80	9.26	13.82	14.49	19.7
MnO	0.36	0.38	0.54	0.41	0.45
MgO	19.31	18.75	15.81	15.85	13.33
CaO	5.43	5.99	5.43	4.93	3.41
Na_2O	0.02	0.02	0.03	0.05	0.05
K_2O	0.00	0.00	0.00	0.00	0.00
Total	99.92	100.18	99.91	100.17	100.15
Cations	Number of cations on the basis of 12 oxygen				
Si	3.000	3.009	3.007	3.007	3.001
Ti	0.005	0.003	0.008	0.006	0.003
Al	1.881	1.961	1.871	1.974	1.989
Cr	0.097	0.008	0.085	0.001	0.002
Fe^{3+}	0.019	0.023	0.034	0.016	0.004
Fe^{2+}	0.498	0.517	0.797	0.857	1.218
Mn	0.022	0.023	0.034	0.025	0.029
Mg	2.060	1.991	1.728	1.719	1.476
Ca	0.416	0.457	0.426	0.384	0.271
Na	0.002	0.002	0.004	0.007	0.006
K	0.000	0.000	0.000	0.000	0.000
Total	7.999	7.994	7.992	7.996	8.001

^{a}Total Fe as FeO

Subgroup B_4, clinopyroxene-amphibole lamellae type garnets (Prp 61–76; Alm 13–27; Grs 6–11 mol%) occur as light-brown-colored crystals with exsolution lamellae of pyroxene, amphibole, rutile, and minor ilmenite. The exsolution lamellae in this subgroup are not as densely packed as in subgroup B_3 garnet (Fig. 1), and occurrences of exsolved amphibole in B_4 are rarer than in subgroups B_1 and B_4. Clinopyroxene and amphibole lamellae tend to occur in the central domains of typical B_4 garnet grains. Thin rims (width ca. 200 μm) lacking any exsolved lamellae phases surround the lamellae-bearing central domains. Exsolved clinopyroxene occurs as needle-shaped (ca. 180×25 μm) and short columnar-shaped (ca. 75×50 μm) crystals and sometime occurs with rutile, ilmenite, and amphibole in composite lamellae. Exsolved clinopyroxene has chemical compositions of Na-bearing diopside to omphacite (Di 60–85 mol%; Na_2O 1.4–5.3 wt%).

Exsolved amphibole in pyrope
Description under microscope
Exsolved amphibole occurs in garnet subgroups B_1, B_3, and B_4. Textures of exsolved amphibole were observed as both (1) monomineralic hexagonal or rhombic prisms and tablets and (2) multimineralic needles or blades composed of amphibole with other exsolved phases. Both types of lamellae are oriented in four directions corresponding crystal directions of garnet host, similar to the first report on amphibole lamellae by Song et al. (2005) that suggested that amphibole lamellae are oriented in four directions corresponding the isometric form {111} of garnet host.

In subgroup B_1, amphibole lamella type garnet, monomineralic prisms and tablets of amphibole occur as coarse-grains (80×20 μm on average) and fine-grains (20×10 μm on average), respectively. Long and short multiphase needles/blades (ca. 350×15 and 25×10 μm, respectively) are composed of amphibole with rutile, ilmenite, srilankite, and apatite.

In subgroup B_3, dense lamellae type garnet, multiphase needles and blades of amphibole occur as long and short (ca. 400×10 and 70×15 μm, respectively) crystals and occur with rutile, ilmenite, srilankite, apatite, and clinopyroxene.

In subgroup B_4, clinopyroxene and amphibole lamellae type garnet, monomineralic prisms/tablets and multiphase needles/blades associated with amphibole have sizes of ca. 80×30 and 400×20 μm, similar to the size of coarse-grained monomineralic/composite exsolved amphibole of B_1 and B_3. Fine-grained monomineralic/composite exsolved amphibole is very rare in subgroup B_4.

Laser Raman study
Exsolved amphibole was identified by laser Raman spectroscopy (Fig. 3). In subgroup B_1, amphiboles of monomineralic prisms/tablets and multiphase needles/blades show Raman peaks at 235, 670, and 3708 cm^{-1} in each spectrum. In subgroup B_3, amphibole has similar Raman peaks at 227, 659, and 3708 cm^{-1}, regardless of occurrence (monomineralic/multimineralic) or morphology (coarse/fine or prism/tablet/needles/blades). In subgroup B_4, coarse-grained amphiboles of monomineralic prisms/tablets and multiphase needles/blades have Raman spectra with peaks at 225, 672, and 3710 cm^{-1}.

Two-dimensional Raman maps were collected in a few cases to show distributions of exsolved amphibole with other exsolved phases in garnet. Raman intensity maps from a garnet crystal of subgroup B_3 in Fig. 4 show the distributions of amphibole (Fig. 4d) and other Ti-bearing phases such as rutile and ilmenite (Fig. 4e). Amphibole occurs as coarse-grained multiphase blades and needles
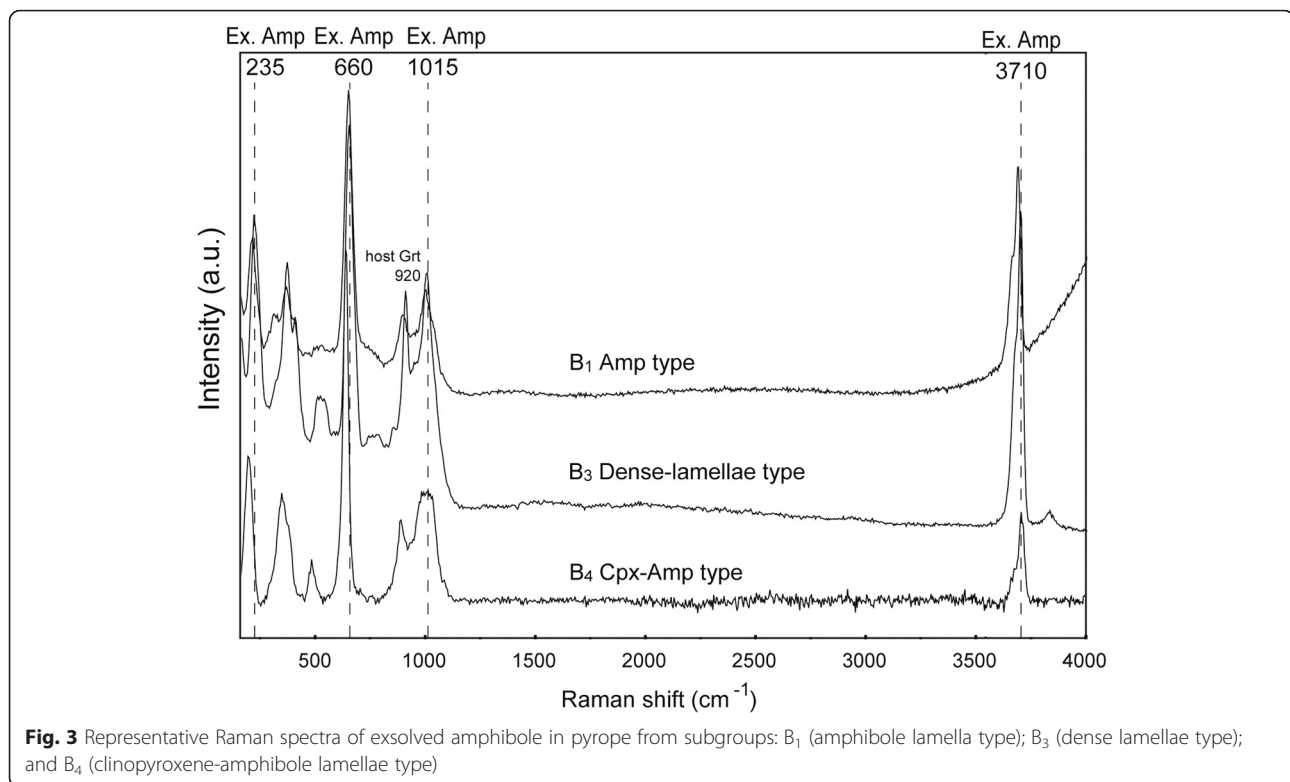
Fig. 3 Representative Raman spectra of exsolved amphibole in pyrope from subgroups: B_1 (amphibole lamella type); B_3 (dense lamellae type); and B_4 (clinopyroxene-amphibole lamellae type)

intergrown together with rutile and ilmenite in this garnet host (Fig. 4). The intergrowth textures suggest that exsolution of amphibole, rutile, and ilmenite occurred at the same stage.

Chemistry

Chemical compositions of exsolved amphibole (>10 μm across) were analyzed with an EMP-WDS. Chemical compositions of exsolved amphibole in subgroups B_1, B_3, and B_4 are listed in Table 3. Based on the EMP analyses, exsolved amphiboles in a given host garnet crystal have homogeneous compositions, but exsolved amphiboles from different host garnets may have different compositions.

In subgroup B_1, amphibole contains up to 1.2 Na atoms per formula unit (apfu, based on 23 oxygen). A representative composition of exsolved amphiboles in B_1 is $Na_{1.10}(Ca_{1.90}Na_{0.10})(Mg_{3.79}Ni_{0.06}Fe_{0.32}Al_{0.79})(Al_{1.95}Si_{6.05})O_{22}(OH_{1.97},Cl_{0.03})$; this is a solid solution of pargasite, $NaCa_2Mg_4AlSi_6Al_2O_{22}(OH)_2$, magnesiohastingsite, $NaCa_2Mg_4Fe^{3+}Si_6Al_2O_{22}(OH)_2$, and magnesiokatophorite, $NaNaCaMg_4AlSi_7AlO_{22}(OH)_2$. According to the classification of Leake et al. (1997), this composition is classified as pargasite.
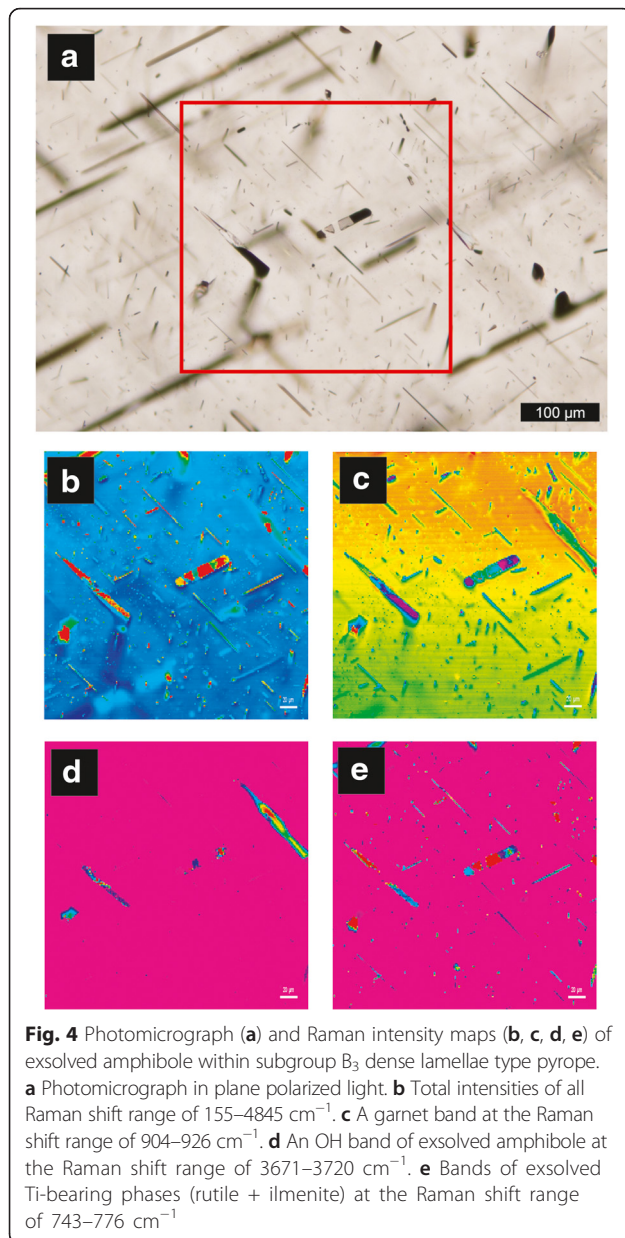
In different garnet grains from subgroup B_3, amphibole shows wider variations of Na (1.0–1.6 apfu) compared to subgroup B_1 amphibole. A representative

composition is $Na_{0.92}(Ca_{1.43}Na_{0.59})(Mg_{3.39}Ni_{0.05}Fe_{0.50}Al_{1.03}Ti_{0.10})(Al_{1.90}Si_{6.10})O_{22}(OH_{1.90},O_{0.10})$. This chemical formula is a solid solution of magnesiotaramite, $Na(CaNa)Mg_3AlFe^{3+}Si_6Al_2O_{22}(OH)_2$, and pargasite.

Exsolved amphibole in subgroup B_4 is characterized by higher Si contents (7.01–7.09 apfu) than the amphibole lamellae in B_1 and B_3. A representative composition is $Na_{0.90}(Ca_{1.40}Na_{0.60})_{2.00}(Mg_{4.30}Fe_{0.28}Al_{0.43})_{5.01}(Al_{0.99}Si_{7.01})_{8.00}O_{22}(OH_{2.00})_2$. This chemical formula is a solid solution of magnesiokatophorite, $Na(NaCa)Mg_4AlSi_7AlO_{22}(OH)_2$, and edenite, $NaCa_2Mg_5Sl_7AlO_{22}(OH)_2$; these endmembers of the amphibole group have slightly high Si contents compared to pargasite (Si 6 apfu based on 23 oxygens). Na contents are similar to those in exsolved amphiboles in subgroups B_1 and B_3.

2D mapping for major/minor elements

X-ray elemental maps of some exsolved amphibole grains and surrounding host garnet were collected from a garnet grain of subgroup B_1. For several elements, garnet host domains surrounding amphibole lamellae show little variation in compositions; however, in some cases, garnet is depleted in Ca, Ti, and Na close to the amphibole lamellae (Fig. 5). These distributions are interpreted as a depletion halos caused by amphibole exsolution from host garnet.

Sakamaki *et al. Progress in Earth and Planetary Science* (2016) 3:20

Page 8 of 17

Fig. 4 Photomicrograph (**a**) and Raman intensity maps (**b**, **c**, **d**, **e**) of exsolved amphibole within subgroup B_3 dense lamellae type pyrope. **a** Photomicrograph in plane polarized light. **b** Total intensities of all Raman shift range of 155–4845 cm^{-1}. **c** A garnet band at the Raman shift range of 904–926 cm^{-1}. **d** An OH band of exsolved amphibole at the Raman shift range of 3671–3720 cm^{-1}. **e** Bands of exsolved Ti-bearing phases (rutile + ilmenite) at the Raman shift range of 743–776 cm^{-1}

Table 3 Representative chemical compositions of exsolved amphibole in garnet subgroups: B_1 (amphibole lamella type), B_3 (dense lamellae type), and B_4 (clinopyroxene-amphibole lamellae type)

	Exsolved amphibole Host garnet: (B) Cr-poor pyrope					
Wt. %	B1		B3		B4	
SiO_2	43.58	42.98	43.90	43.62	50.24	50.51
TiO_2	0.35	0.33	1.09	0.97	0.23	0.19
Al_2O_3	16.13	16.38	18.25	16.71	8.65	8.93
Cr_2O_3	0.12	0.14	0.07	0.00	0.19	0.16
FeO^a	2.21	2.49	3.97	3.75	2.40	2.38
CaO	12.64	12.37	9.33	11.54	9.37	9.12
MnO	0.03	0.00	0.03	0.02	0.00	0.02
MgO	18.00	18.12	15.71	17.18	20.67	20.48
NiO	0.76	0.38	0.36	0.34	0.13	0.09
Na_2O	4.26	3.84	5.62	3.81	5.55	5.35
K_2O	0.01	0.00	0.02	0.00	0.31	0.30
Cl	0.10	0.02	0.00	0.00	0.02	0.04
Total	98.18	97.05	98.36	97.94	97.77	97.57
Cations	Number of cation based on 23 oxygen					
Si	6.137	6.104	6.145	6.142	7.006	7.039
Ti	0.037	0.036	0.115	0.103	0.024	0.020
Al	2.677	2.742	3.011	2.774	1.422	1.467
Cr	0.013	0.016	0.008	0.000	0.021	0.018
Fe^{2+}	0.260	0.296	0.465	0.442	0.280	0.277
Ca	1.907	1.882	1.399	1.741	1.400	1.362
Mg	3.778	3.836	3.278	3.606	4.297	4.254
Mn	0.003	0.000	0.004	0.002	0.000	0.002
Ni	0.087	0.044	0.041	0.038	0.014	0.010
Na	1.163	1.057	1.525	1.040	1.501	1.446
K	0.001	0.000	0.004	0.000	0.054	0.053
Total	16.064	16.011	15.995	15.889	16.023	15.955
Cl	0.024	0.005	0.000	0.000	0.004	0.009

[a]Total Fe as FeO

IR spectra and water contents of pyrope
Group A: Cr-rich pyrope
IR spectra obtained from group A, Cr-rich pyrope crystals stop, have dominant absorption bands with peaks near 3575 cm^{-1} and minor bands at 3660–3680 cm^{-1} (Fig. 6 and Table 4). The dominant peaks near 3575 cm^{-1} are similar to an OH band in pyrope reported by Aines and Rossman (1984). OH concentrations in the host garnet range from below the detection limit (1 ppmw) to 115 ppmw H_2O (Fig. 8).

Group B: Cr-poor pyrope
Obtained IR spectra show strong absorption bands near 3575 cm^{-1} and relatively weak bands at 3660–3680 cm^{-1},

both associated with structural OH in host garnet (Figs. 6 and 7; Table 4; see Aines and Rossman 1984). These two IR bands are similar to OH bands in group A garnet. Broad bands at ca. 3400 cm^{-1} were sometimes detected in subgroups B_1 and B_2. These broad bands are probably caused by molecular H_2O in fluid inclusions (e.g., Libowitzky and Rossman 1997). Sharp bands at ca. 3710 cm^{-1}, apparently due to OH in amphibole, were identified in subgroups B_1, B_3, and B_4. OH concentrations in host garnet are estimated at as follows: B_1 3–42 ppmw H_2O, B_2 27 and 101 ppmw (two grains analyzed), B_3 4–10 ppmw, and B_4 2 ppmw (one grain analyzed; see Fig. 8). Garnets from subgroups B_1, B_3, and B_4, all characterized by

Sakamaki *et al. Progress in Earth and Planetary Science* (2016) 3:20
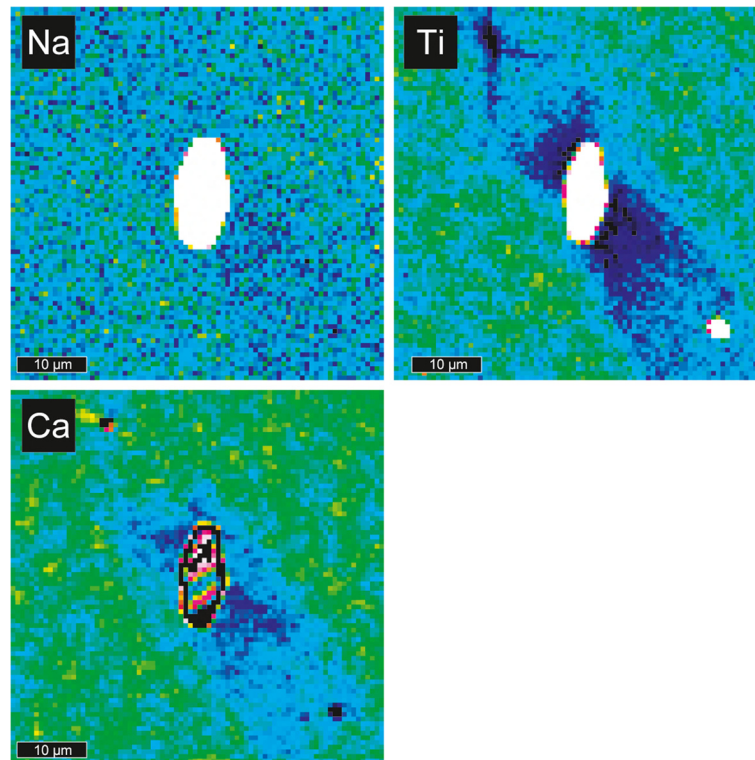
Page 9 of 17

Fig. 5 X-ray images for Na-Kα, Ti-Kα, and Ca-Kα of exsolved amphibole in B_3 dense lamellae type garnet

amphibole-bearing exsolution lamellae, have lower water concentrations than group A and subgroup B_2 garnets, which do not have exsolved amphibole.

Discussion

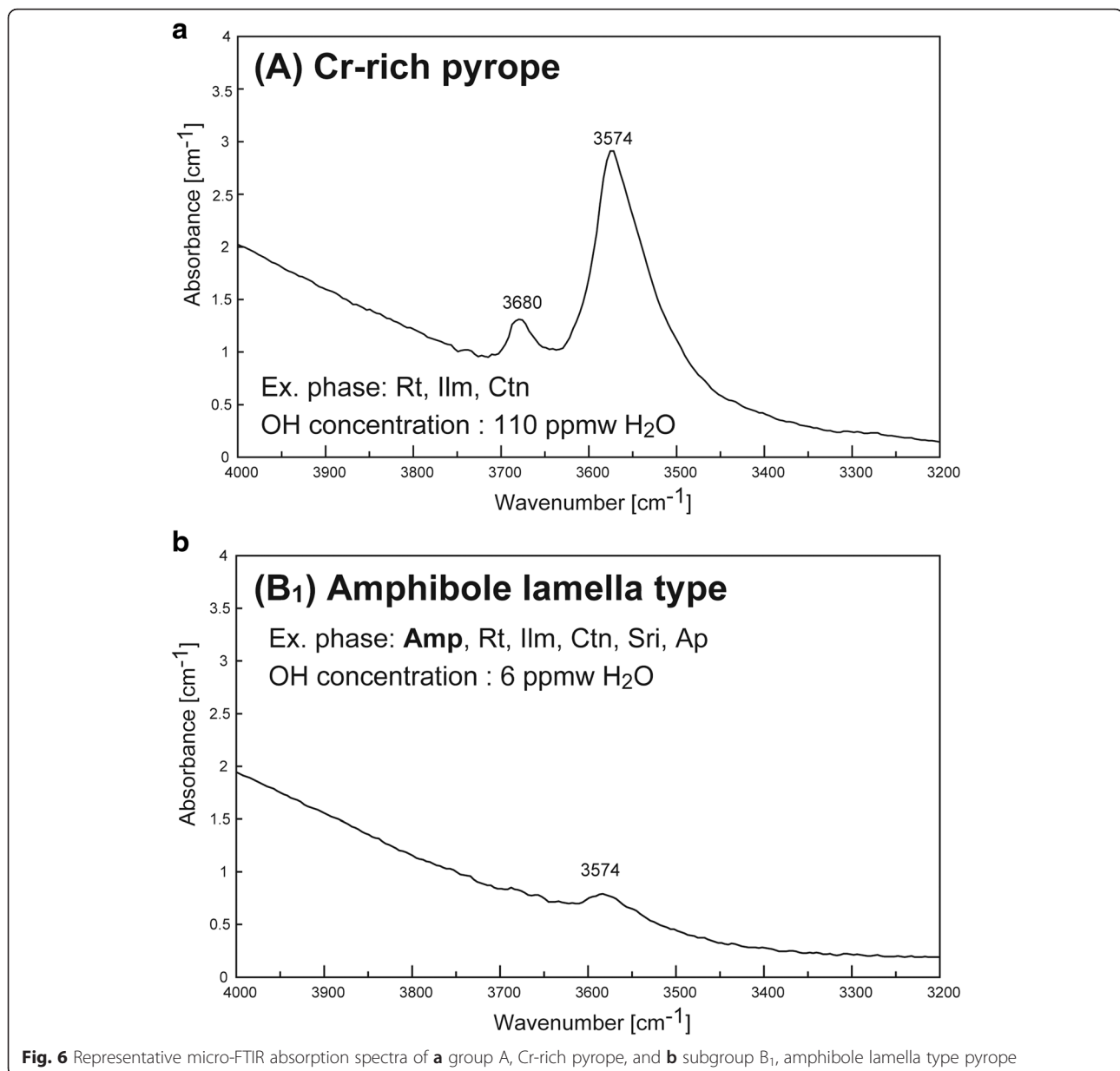### Protoliths of garnet-bearing rocks underneath the Colorado Plateau

Classification of kimberlitic garnet xenocrysts has been conducted based on chemistry and inclusions for many years (e.g., Dawson and Stephens 1975; Danchin and Wyatt 1979; Schulze 2003; Grütter et al. 2004). Schulze (2003) compiled published analyses of garnets from ultramafic xenoliths in kimberlite and proposed a method for distinguishing mantle vs. crustal origins of garnets based on Mg/(Mg + Fe) and Ca/(Ca + Mg). According to results of Schulze (2003), garnet with Mg/(Mg + Fe) of 0.5–1 and Ca/(Ca + Mg) of 0.1–0.9 probably has a mantle origin. Most analyses of the group A [Mg/(Mg + Fe) = 0.79–0.85, Ca/(Ca + Mg) = 0.09–0.14] and group B [Mg/(Mg + Fe) = 0.56–0.85, Ca/(Ca + Mg) = 0.08–0.65] pyropes of this study indicate mantle origins based on the criteria of Schulze (2003) (see their Fig. 1).

Grütter et al. (2004) proposed that Mg, Ca, Fe, Cr, and Ti contents of mantle-derived garnet can be used to distinguish 13 compositional types of garnet, each associated with a likely mantle rock-type. The group A pyrope of this study has a composition (Pyp$_{67-74}$,

4–6 wt% CaO, and up to 6.4 wt% Cr_2O_3) similar to garnet from lherzolite or Fe-rich pyroxenite, based on the classification of Grütter et al. (2004), see CaO vs Cr_2O_3 diagram in Fig. 7). The inclusion assemblage in group A garnet is olivine-orthopyroxene-clinopyroxene, each occurring in similar abundances (Table 1). These clues suggest that the group A pyrope crystals came from lherzolite or olivine-websterite.

Chemical compositions of group B are characterized by low Cr contents and wide variations of Mg and Ca compared to group A (Fig. 2b). The compositions of subgroup B_1 (Pyp$_{49-66}$, 5–10 wt% CaO, and up to 0.5 wt% Cr_2O_3) and B_3 (Pyp$_{54-72}$, 4–6 wt% CaO, and up to 0.6 wt% Cr_2O_3) are similar to those of garnet in pyroxenite (e.g., mantle eclogite, pyroxenite, and websterite) or the low-Ca pyroxenite in Grütter et al. (2004). The trapped inclusions in subgroups B_1 and B_3 are dominantly clinopyroxene, whereas olivine and orthopyroxene were not identified at all (Table 1). Therefore, the host rocks of subgroups B_1 and B_3 are probably garnet-bearing clinopyroxenites.

Subgroup B_4 pyrope crystals have compositions that are relatively poor in Ca and Cr (Pyp$_{61-76}$, 3–4 wt% CaO, and up to 0.6 wt% Cr_2O_3) compared to subgroups B_1 and B_3 (Fig. 2b). The B_4 pyrope compositions are similar to garnets from low-Ca pyroxenite (Grütter et al. 2004). In addition, subgroup B_4 garnet contains trapped

Sakamaki *et al. Progress in Earth and Planetary Science* (2016) 3:20

Page 10 of 17

Fig. 6 Representative micro-FTIR absorption spectra of **a** group A, Cr-rich pyrope, and **b** subgroup B$_1$, amphibole lamella type pyrope

inclusions of olivine and orthopyroxene, but clinopyroxene inclusions were not identified (Table 1). This inclusion assemblage combined with the Ca-, Cr-poor compositions suggest that subgroup B$_4$ garnet likely originates from garnet-bearing olivine orthopyroxenite or harzburgite.

Subgroup B$_2$ has slightly higher Cr contents (Pyp$_{49-68}$, 4–7.5 wt% CaO, and 1–2 wt% Cr$_2$O$_3$) than subgroups B$_1$, B$_3$, and B$_4$ (Fig. 2b). The composition of subgroup B$_2$ garnet is similar to the compositions of Fe-rich pyroxenitic garnet reported by Grütter et al. (2004). Subgroup B$_2$ garnet contains trapped inclusions of olivine, orthopyroxene, clinopyroxene, and fluid inclusions (Table 1). We infer that the host rock of subgroup B$_2$

garnet is probably hydrated garnet-bearing lherzolite or olivine-websterite.

Group A (lherzolitic or websteritic) garnet is the most abundant type of garnet that we identified at Garnet Ridge. Garnet-lherzolite and olivine-websterite are therefore considered to be dominant and typical garnet-bearing constituents of upper mantle underneath the Colorado Plateau. The group A garnet has a limited chemical variation in Mg-Fe-Ca contents, whereas each subgroup of group B (pyroxenitic origins) has a wider chemical range (Fig. 2a); some garnets of group B have Mg-Fe-Ca contents that overlap with group A garnet but many in group B have more Ca- and/or Fe-rich compositions than the concentrated chemical range of group A (Fig. 2).

Sakamaki *et al. Progress in Earth and Planetary Science* (2016) 3:20

Page 11 of 17

Table 4 Micro-FTIR analyses of pyrope from Garnet Ridge

Chemistry						Micro-FTIR analysis				
	Classification	Sample no.	Pyp$_{(mol\%)}$	Cao$_{(wt\%)}$	Cr$_2$O$_3$ $_{(wt\%)}$	Band positions (cm^{-1})			Int. Abs. [a](cm^{-1})	OH contents (ppmw)
A	Cr-rich pyrope	S1_Pr1	69	5.5	2.2			3573	41.3	24
A	Cr-rich pyrope	S1_Pr2	70	5.5	2.3		3678	3573	83.7	48
A	Cr-rich pyrope	S1_Pr3	70	4.9	2.8		3678	3572	164.9	95
A	Cr-rich pyrope	S2_Pr1	69	5.3	5.1		3673	3571	136.8	78
A	Cr-rich pyrope	S2_Pr2	69	5.2	2.3		3680	3571	60.3	35
A	Cr-rich pyrope	S2_R3	67	5.1	2.3		3675	3571	201.0	115
B$_1$	Amp type	S1_Br1	59	7.6	0.0			3575	41.5	24
B$_1$	Amp type	S2_Br2	49	7.6	0.0		3674	3578	73.3	42
B$_1$	Amp type	S4_Br1	65	7.3	0.1			3574	10.7	6
B$_1$	Amp type	S6_Br1	62	7.0	0.1			3569	4.8	3
B$_2$	Ilm-only type	S2_Br2	57	5.6	1.8		3666	3573	176.7	101
B$_2$	Ilm-only type	S5_Br2	60	6.3	1.8		3653	3549	46.9	27
B$_3$	Dense lamellae type	0909B_Bl3_1	73	4.6	0.3			3580	6.7	4
B$_3$	Dense lamellae type	0909B_Bl3_2	69	5.3	0.4	3718$_{(Amp)}$		3570	17.2	10
B$_3$	Dense lamellae type	0909B_Bl3_3	69	5.1	0.3			3572	7.5	4
B$_3$	Dense lamellae type	0909B_Bl3_4	60	5.1	1.0	3712$_{(Amp)}$	3684$_{(Amp)}$	3579	12.4	7
B$_4$	Cpx-Amp type	S3_Br1	66	4.8	0.5			3569	4.0	2

[a]Integrated absorbance of OH bands of garnet host

The wide chemical ranges of Ca and Fe in group B show linear variations in Mg-Fe-Ca contents. In general, such linear chemical variations are interpreted as mixtures of two different compositions. Therefore, group A (typical lherzolitic/olivine-websteritic) pyrope may represent a primitive, Mg-rich endmember of the garnets at Garnet Ridge. The Ca- and Fe-rich compositional variations of the group B are likely products of interaction between the typical lherzolitic/olivine-websteritic garnet and Ca/Fe-rich media such as fluids (Fig. 9). A few garnet crystals of group A and some garnet in subgroups B$_2$ and B$_3$ have volatile-bearing inclusions of dolomite, magnesite, apatite, and chlorite (Table 1) and contain significant amounts of OH up to 115 ppmw in group A and up to 101 ppmw in the group B. These clues of volatile, H$_2$O-rich environments suggest that the chemical changes from the group A garnet to more Ca/Fe-rich compositions were caused by fluid-mediated mantle metasomatism. During metasomatism, the host rocks of group B transformed from typical mantle lherzolites and olivine-websterites to pyroxenitic rocks (e.g., Sapienza et al. 2009; Vrijmoed et al. 2013).

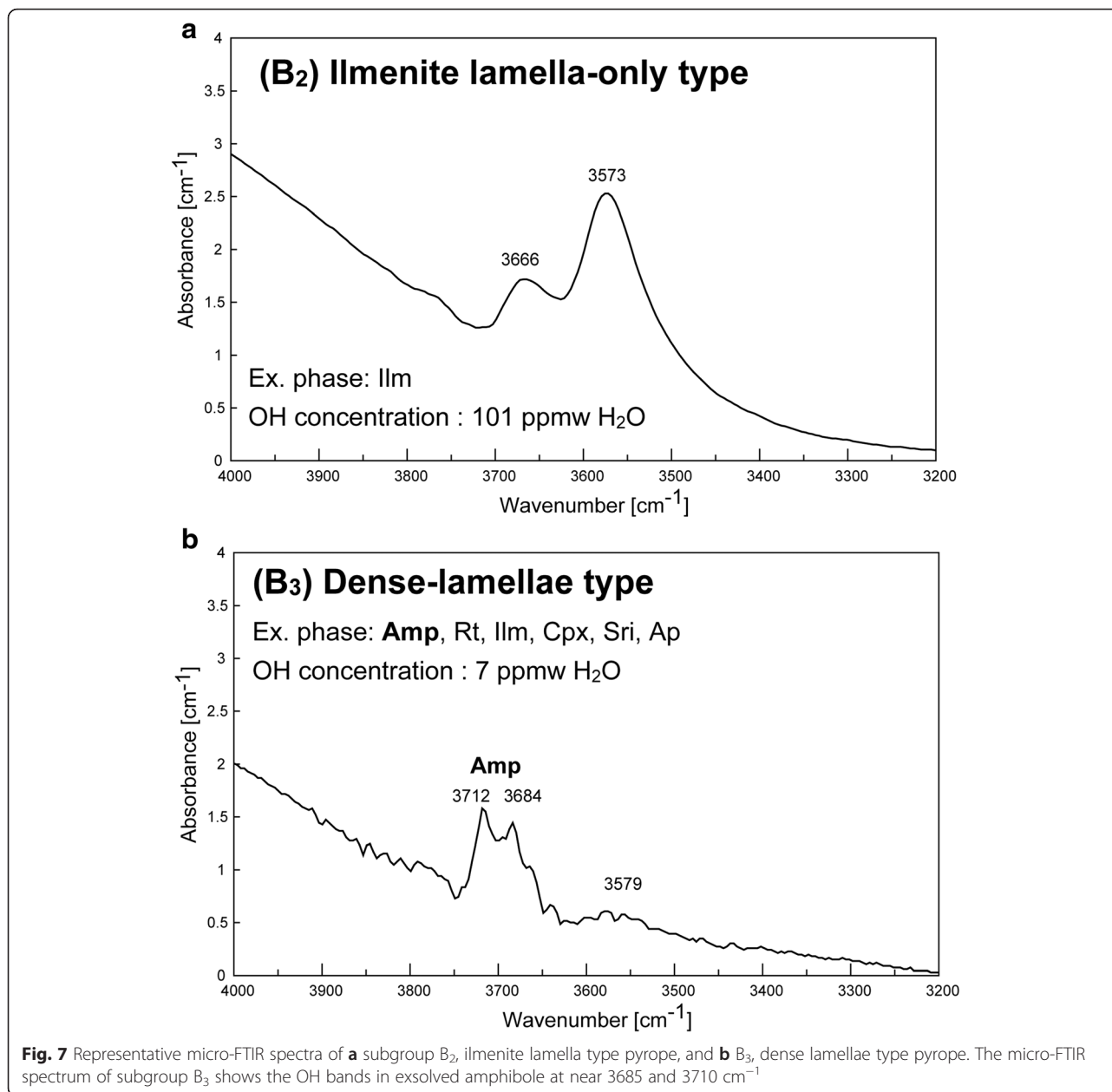### Exsolved amphibole-bearing garnet after hydrous Na-garnet

The following points are critical for determining the origin of amphibole grains in pyrope from Garnet Ridge: (1) preferred orientation of amphibole grains controlled by crystal orientations of the host garnet; (2) depletion haloes of Na, Ca and Ti in the host garnet surrounding amphibole grains; and (3) low OH contents in amphibole-bearing garnet host. Considering these observations, we infer that the oriented amphibole inclusions in pyrope crystals formed by exsolution from precursor Na- and OH-rich garnet. Amphibole exsolution from garnet is rarely reported; we are aware of only one previous report on amphibole exsolution from North Qaidam UHP metamorphic belts, northern Tibet, NW China (Song et al. 2005).

Exsolved amphiboles in pyrope from Garnet Ridge contain significant amounts of Na (up to 1.6 apfu on the basis of 23 oxygen), and their chemistries approximate pargasite, NaCa$_2$Mg$_4$AlSi$_6$Al$_2$O$_{22}$(OH)$_2$. The chemical formula of precursor garnet prior to amphibole exsolution was a solid solution that included the components necessary to exsolve amphibole. The precursor garnet before amphibole exsolution must have had a "hydrous Na-garnet" component, such as (Mg, Na$_x^+$)$_{3}$(Al$_{2-x}$, Mg$_x$)$_2$Si$_3$O$_{12-2x}$(OH)$_{2x}$. This garnet was broken down by a reaction similar to the following:

$$(Mg, Ca, Na_x)_3(Al_{2-x}, Mg_x)_2Si_3O_{12-2x}(OH)_{2x}$$
$$\rightarrow x \ NaCa_2(Mg_4Al)Si_6Al_2O_{22}(OH)_2$$
$$+(1-2x)(Mg, Ca)Al_2Si_3O_{12}.$$
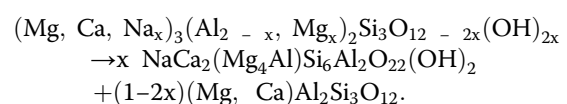
The pargasite stability field is limited to pressures <3 GPa (Green 1973), indicating that breakdown of hydrous Na-garnet and formation of exsolved

Sakamaki *et al. Progress in Earth and Planetary Science* (2016) 3:20

Page 12 of 17

Fig. 7 Representative micro-FTIR spectra of **a** subgroup B₂, ilmenite lamella type pyrope, and **b** B₃, dense lamellae type pyrope. The micro-FTIR spectrum of subgroup B₃ shows the OH bands in exsolved amphibole at near 3685 and 3710 cm^{-1}

pargasite occurred at such relatively low-pressure conditions.

The importance of minor amounts of Na and OH in garnet as UHP indicators has been suggested in previous studies (e.g., Irifune et al. 1989; Bell and Rossman 1992a). The first report on Na-rich garnet is from a majoritic garnet with 1.08 wt% Na₂O that occurs as an inclusion in kimberlitic diamond (Moore and Gurney 1985). At present, reports on observed occurrences of Na-rich garnet are limited to UHP metamorphic rocks and inclusions in diamond from kimberlite pipes (Sobolev and Lavrent'ev 1971; Bishop et al. 1978; Enami et al. 1995; Song et al. 2005).

Previous UHP experiments have demonstrated that Na can be incorporated in garnet structures together with other elements such as excess Si, Ti, and P at UHP conditions to form Na-Si ($Na_2MgSi_5O_{12}$; see Gasparik 1989 and Bobrov et al. 2008), Na-Ti ($Na_2CaTi_2Si_3O_{12}$; see Ringwood and Lovering 1970), and Na-P ($Na_3Al_2P_3O_{12}$; see Brunet et al. 2006) components of garnet. Hydrous Na-garnet, $(Mg, Ca, Na_x)_3(Al_{2-x}, Mg_x)_2Si_3O_{12-2x}(OH)_{2x}$, described as precursor composition in this paper has not been identified in UHP experiments as of yet and is a solid solution with a previously unidentified Na-bearing hydrous endmember of the garnet group at UHP conditions.

Sakamaki *et al. Progress in Earth and Planetary Science* (2016) 3:20

Page 13 of 17
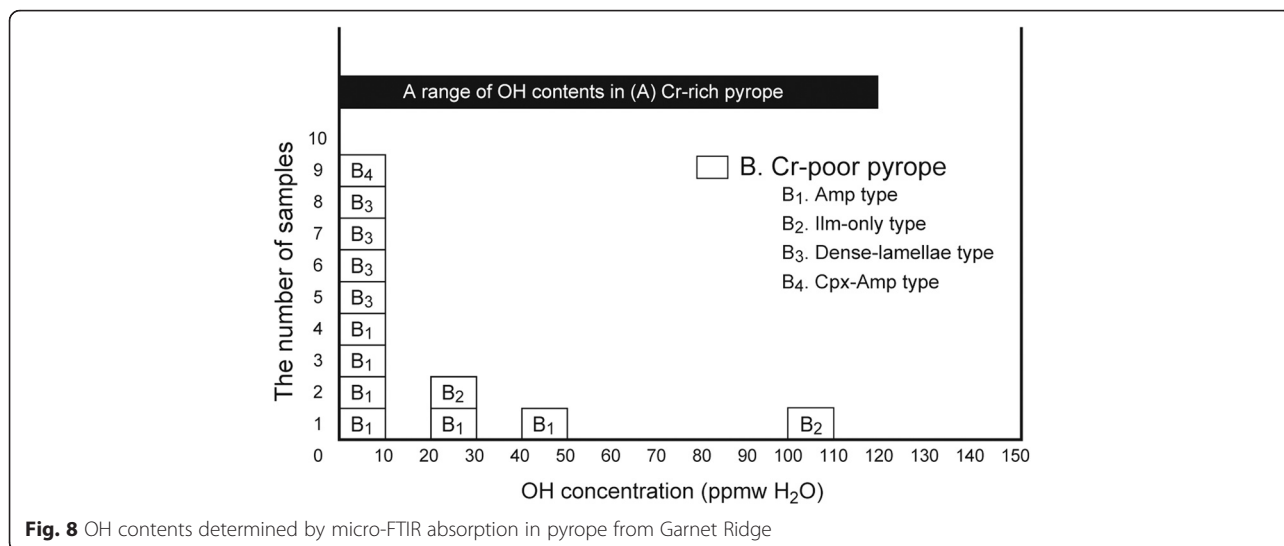
Fig. 8 OH contents determined by micro-FTIR absorption in pyrope from Garnet Ridge

There are a few experimental studies examining stability of Na-bearing garnet. For example, Ringwood and Lovering (1970) conducted the first synthesis of Na-bearing garnet and demonstrated that the minimum pressure to synthesize Na-bearing garnet (1.2 wt% Na_2O) from a mixture of clinopyroxene and ilmenite (2:3) is approximately 105 kb at 1000 °C. In UHP experiments conducted by Gasparik (1989), Na-rich majorite garnet was synthesized at 133 kbar and 1650 °C with the composition $En_{42}Di_9Jd_{49}$; for pyroxene with starting compositions with Jd <60 mol%; pressures in excess of 140 kbar (at 1500 °C) were required to form garnet with Na-bearing pyroxene compositions. In UHP experiments in the $Mg_3Al_2Si_3O_{12}$–$Na_2MgSi_5O_{12}$ system conducted by Bobrov et al. (2008), Na-rich garnet with 1.52 wt% Na_2O (6 mol% $Na_2MgSi_5O_{12}$) was synthesized at 8.5 GPa and 1760 °C and demonstrated that Na concentrations in garnet increase with increasing pressure or with decreasing temperature. Since direct experimental data on hydrous Na-garnet are lacking, its stability limit is unclear. Considering the experimentally determined conditions of anhydrous Na-bearing garnet and the natural occurrence of Na-rich garnets in UHP settings, we conclude that hydrous Na-garnet must be stable at least in UHP conditions.
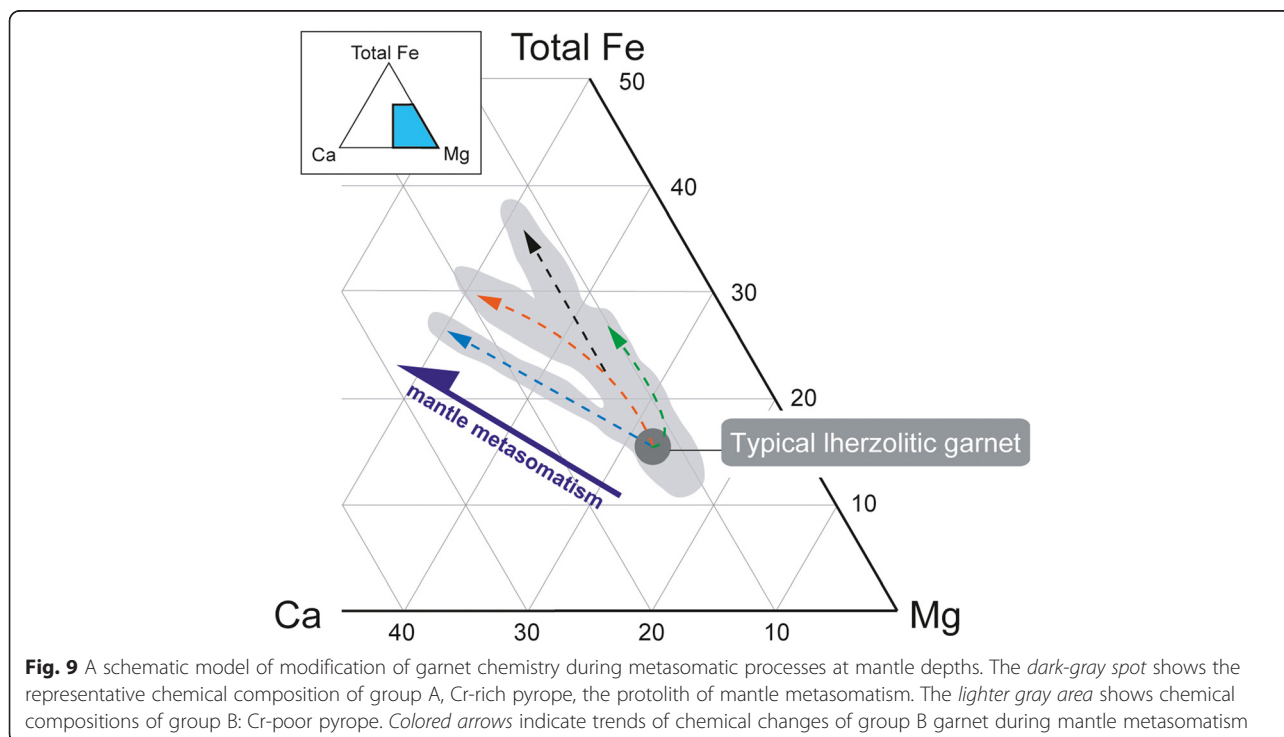
Fig. 9 A schematic model of modification of garnet chemistry during metasomatic processes at mantle depths. The *dark-gray spot* shows the representative chemical composition of group A, Cr-rich pyrope, the protolith of mantle metasomatism. The *lighter gray area* shows chemical compositions of group B: Cr-poor pyrope. *Colored arrows* indicate trends of chemical changes of group B garnet during mantle metasomatism

Sakamaki *et al. Progress in Earth and Planetary Science* (2016) 3:20

Page 14 of 17

We estimated growth conditions of hydrous Na-garnet from subgroup B_4, clinopyroxene and amphibole lamellae type, in which exsolved amphibole coexists with exsolved Na-bearing clinopyroxene (up to 5.3 wt% Na_2O). The presence of Na-bearing pyroxene exsolution lamellae suggests that precursor garnet had excess Si as a characteristic of majorite garnet under UHP conditions (e.g., Moore and Gurney 1985; Van Roermund et al. 2001). The coexistence of exsolved amphibole and clinopyroxene in single garnet grains indicates that Na-, OH-, and Si-rich components were dissolved in the precursor garnet. As a first step toward estimating growth conditions of the garnet, we recalculated an original excess Si component of garnet based on modes and compositions of clinopyroxene lamellae and surrounding garnet host in a representative domain of B_4 garnet. The modes were estimated from 1000 μm × 1000 μm elemental maps. The mode of clinopyroxene lamella in this area reaches 1.7 %, resulting in a calculated excess Si content of 0.017 apfu (based on 12 oxygen). For garnet with excess Si, charge balance can be maintained by paired substitution of divalent cations (M^{2+}), such as Mg, for trivalent Al in the six-coordinated site of garnet structure (Ringwood 1967); thus, the B_4 garnet described above probably had a six-coordinated site consisting of $M^{2+}_{0.017}Al_{1.966}Si_{0.017}$ apfu (12 oxygen basis) prior to exsolution of clinopyroxene. Gasparik (1990) conducted experiments in the system, $CaO\text{-}MgO\text{-}Al_2O_3\text{-}SiO_2$, and demonstrated that Al contents in garnet decrease with increasing pressure due to formation of majoritic garnet. According to his results, the garnet with $Al_{1.966}$ apfu is stable at pressures of 8 GPa at 1000 °C, 7 GPa at 1200 °C, and 6 GPa at 1400 °C. These results suggest that our hydrous Na-garnet formed in a depth range of 200–250 km, suggesting origin in asthenospheric mantle (Condie 2005; O'Reilly and Griffin 2006).

Trace amounts of OH are identified in garnet from kimberlitic xenoliths/xenocrysts and UHP metamorphic rocks; (1) 2–163 ppmw in mantle-delivered pyrope (Matsyuk et al. 1998); (2) 92 to 1735 ppmw in eclogitic garnet from Dabieshan (Xia et al. 2005); and (3) up to ca. 1500 ppmw in the Kokchetav garnet-clinopyroxene rocks (Sakamaki et al. 2014). Importance of garnet as an OH reservoir in the upper mantle should not be ignored. A few UHP experiments demonstrated that OH solubilities in garnet were controlled by pressure conditions; Lu and Keppler (1997) ascertained that OH solubility in pyrope increases with pressure <10 GPa from 73.5 ppmw (at 15 kbar, 1000 °C) to 198.9 ppmw (at 100 kbar, 1000 °C). Withers et al. (1998) showed that OH solubility in pyrope increase with pressure <6 GPa from 140 ppmw (at 20 kbar, 1000 °C) to 960 ppmw (at 60 kbar, 1000 °C) but then decreases to 0 ppmw until 13 GPa; their results are different from those of Lu and Keppler

(1997) at pressures >7 GPa. In either case, OH solubility in pyrope increases with pressure up to 6 GPa.

In this study, the OH contents in group A garnet range from below the detection limit (<1 ppmw) to 115 ppmw. Such OH contents in group A garnet are typical of OH contents in mantle-delivered pyrope; for example, less than 2 ppmw up to 163 ppmw in mantle pyrope from kimberlite pipes of the Siberian platform (Matsyuk et al. 1998) and less than 1 ppmw up to 135 ppmw in subcontinental lithosphere delivered garnet from 18 kimberlite pipes in southern Africa (Bell and Rossman 1992b). In contrast, exsolved amphibole-bearing garnet, subgroups B_1 (3–42 ppmw), B_3 (4–10 ppmw), and B_4 (2 ppmw), have significantly lower H_2O contents than those in the lherzolitic or websteritic garnet of group A (up to 115 ppmw) and the exsolved amphibole-free subgroup B_2 (27 and 101 ppmw). The lower H_2O contents in amphibole-bearing garnets are interpreted as a consequence of transfer of OH from host garnet to amphibole during exsolution.

Growth conditions of hydrous Na-garnet

Na is considered to be a minor element in the upper mantle; Na contents in average mantle peridotite (pyrolite) were estimated as no higher than 0.4 wt% Na_2O by Ringwood (1975). Bishop et al. (1978) describe garnet-lherzolite xenoliths in African kimberlites containing Na-poor (0.017–0.038 wt% Na_2O) garnet coexisting with Na-rich clinopyroxene (2.01–4.66 wt% Na_2O), Na-poor orthopyroxene (0.053–0.181 wt% Na_2O), and Na-poor olivine (0–0.013 wt% Na_2O). The results of Bishop et al. (1978) suggest that most of Na is partitioned into clinopyroxene rather than garnet at upper mantle conditions. It is likely that the absence of clinopyroxene is one of the keys for growth of Na-rich garnet. Among our hydrous Na-garnet (subgroups B_1, B_3, and B_4), subgroup B_4 garnet apparently formed without coexisting with clinopyroxene (see Table 1). In contrast, for subgroups B_1 and B_3, the occurrence of trapped inclusions of clinopyroxene in garnet (Table 1) indicates that clinopyroxene was present during garnet growth. The second key for growth of Na-rich garnet is perhaps locally high concentration of Na in the upper mantle; subgroups B_1 and B_3 garnet likely formed under Na-concentrated environments at upper mantle depths.

Growth conditions of hydrous Na-garnet are considered dependent on the following conditions: (1) 200–250 km depth, in asthenospheric mantle; (2) pyroxenitic host rocks; (3) volatile-rich metasomatic environments; and (4) Na-enriched environments. The linear variations in Mg-Fe-Ca contents (Fig. 9) suggest that initial, pre-metasomatic garnets had Mg-rich compositions typical of lherzolitic garnet. We infer that hydrous Na-garnet formed in pyroxenites that

Sakamaki *et al. Progress in Earth and Planetary Science* (2016) 3:20

Page 15 of 17

are products of metasomatism of typical mantle lherzolites/westerites by infiltration of Na-rich aqueous fluids. The most likely sources of Na-rich aqueous fluids are oceanic plates subducted into the upper mantle, because Na contents in oceanic crust (2–3 wt% Na_2O; Sun et al. 1979) are much higher than those in typical mantle pyrolite (0.4 wt% Na_2O; Shido et al. 1971). During ocean-floor metamorphism when crust is produced at oceanic ridges, the oceanic crust and sublithospheric mantle of oceanic plates are typically enriched with water. Water contents increase from <1 wt% H_2O in primitive oceanic crust (Poli and Schmidt 1995) to up to ca. 5 wt% H_2O in hydrated oceanic crust (Peacock 1993). During subduction, this hydrated, Na-enriched oceanic crust is transported to the upper mantle, providing a source material for the formation of hydrous Na-garnet at upper mantle conditions (e.g., Katayama et al. 2006).

Hydrous subducted oceanic plates are eventually dehydrated by breakdown of hydrous phases such as serpentine, lawsonite, amphiboles, and micas, and as a result, H_2O-rich fluids are released in the deep upper mantle (e.g., Poli and Schmidt 1995). Significant amounts of Na are likely dissolved to aqueous fluids released from hydrous subducted oceanic plates. Such Na-rich aqueous fluids could ascend to overlying mantle peridotites and cause metasomatism of primitive mantle lherzolite and websterite (the host rock of group A garnet in this study) at depths >200 km. During mantle metasomatism, typical lherzolite and websterite may transform to pyroxenites. Hydrous Na-garnet probably forms in such metasomatized pyroxenites under Na-rich aqueous fluids environments.

Until at least 30 Ma when kimberlitic volcanism occurred at Garnet Ridge (Smith et al. 2004), the oceanic Farallon plate subducted beneath the west coast of North America and apparently extended at a shallow subduction angle to the mantle region below the Colorado Plateau (Coney and Reynolds 1977; Bunge and Grand 2000). Is the Farallon Plate the source of Na-rich aqueous fluids that caused mantle metasomatism of peridotites underneath the Colorado Plateau? According to the petrologic and geochronologic work of Usui et al. (2003), just before eruption of kimberlite 30 Ma, oceanic crust of the Farallon Plate existed at depths of 100–150 km (3–5 GPa; 560–700 °C). Even if the Farallon Plate was dehydrated underneath the Colorado Plateau, Na-rich aqueous fluids released from the Farallon Plate probably ascended to overlying shallow mantle (Schulze et al. 2015). In such shallow mantle conditions (<100 km), pargasite is a more stable hydrous Na-bearing phase than hydrous Na-garnet (Green 1973). Consequently, we suggest that dehydration of the Farallon Plate is not the origin of Na-rich aqueous fluid to form hydrous Na-garnet.

Instead, the hydrous Na-garnet may have grown in the asthenospheric mantle underneath the Farallon Plate. According to estimated growth conditions of subgroup B_4 garnet at least 6 GPa, 1200 °C to 8 GPa,1000 °C, the hydrous Na-garnet must have grown at depths >200 km, probably in asthenospheric mantle A possible source of Na-rich aqueous fluids causing mantle metasomatism in asthenospheric mantle is ancient deeply subducted oceanic crust before subduction of the Farallon Plate.

Na and OH in pyrope garnet from the Colorado Plateau indicate not only UHP conditions of upper mantle origin, but also have important implications for the history of mantle metasomatism related to mantle dynamics, such as plume tectonics and subduction of oceanic plates underneath the North American Plate. Future research on direct age dating and trace components in pyrope garnets from the Navajo Volcanic Field will be necessary for deciphering the origin of the Na-rich hydrous garnets and their relation to the geologic history of formation of the Colorado Plateau.

Conclusions

Pyrope xenocrysts from Garnet Ridge are classified into two groups: group A, Cr-rich pyrope; and group B, Cr-poor pyrope. The group B is subdivided into four subgroups: B_1 amphibole lamella type; B_2 ilmenite lamella only type; B_3 dense lamellae type; and B_4 clinopyroxene-amphibole lamellae type. Exsolved amphibole occurs in B_1, B_3, and B_4 as monomineralic prisms/tablets and as multimineralic needles/blades with other exsolved phases such as rutile, ilmenite, srilankite, apatite, and clinopyroxene. Exsolved amphibole mainly has pargasitic compositions.

OH contents in exsolved amphibole-bearing garnet host (subgroups B_1, B_3, and B_4) are significantly lower than those of exsolved amphibole-free garnet (group A and subgroup B_2). This suggests a loss of OH in garnet host during amphibole exsolution.

Amphibole exsolution in pyrope crystals resulted from breakdown of hydrous Na-garnet components in precursor garnet at <3 GPa during decompression. Hydrous Na-garnet was apparently formed by metasomatism of mantle peridotite caused by infiltration of Na-rich fluids in asthenospheric mantle (at least 200–250 km) under the Colorado Plateau. Metasomatic Na-rich fluids probably originated from dehydration of ancient oceanic crust that was subducted before subduction of the Farallon Plate.

Sakamaki *et al. Progress in Earth and Planetary Science* (2016) 3:20

Page 16 of 17

References

Aines RD, Rossman GR (1984) The hydrous component in garnets: pyralspites. Am Mineral 69:1116–1126

Bell DR, Rossman GR (1992a) Water in earth's mantle: the role of nominally anhydrous minerals. Science 255:1391–1397. doi:10.1126/science.255.5050.1391

Bell DR, Rossman GR (1992b) The distribution of hydroxyl in garnets from the subcontinental mantle of southern Africa. Contrib Mineral Petrol 111:161-178. doi:10.1007/BF00348949

Bishop FC, Smith JV, Dawson JB (1978) Na, K, P and Ti in garnet, pyroxene and olivine from peridotite and eclogite xenoliths from African kimberlites. Lithos 11:155–173. doi:10.1038/35012586

Bobrov AV, Litvin YA, Bindi L, Dymshits AM (2008) Phase relations and formation of sodium-rich majoritic garnet in the system $Mg_3Al_2Si_3O_{12}$–$Na_2MgSi_5O_{12}$ at 7.0 and 8.5 GPa. Contrib to Mineral Petrol 156:243–257. doi:10.1007/s00410-008-0283-3

Brunet F, Bonneau V, Irifune T (2006) Complete solid-solution between $Na_3Al_2(PO_4)_3$ and $Mg_3Al_2(SiO_4)_3$ garnets at high pressure. Am Mineral 91:211–215. doi:10.2138/am.2006.2053

Bunge HP, Grand SP (2000) Mesozoic plate-motion history below the northeast Pacific Ocean from seismic images of the subducted Farallon slab. Nature 405:337–340. doi:10.1038/35012586

Condie KC (2005) TTGs and adakites: are they both slab melts? Lithos 80:33–44. doi:10.1016/j.lithos.2003.11.001

Coney PJ, Reynolds SJ (1977) Cordilleran benioff zones. Nature 270:403–406. doi:10.1038/275464a0

Danchin RV, Wyatt BA (1979) Statistical cluster analysis of garnets from kimberlites and their xenoliths. Kimberlite Symposium II., pp 22–27

Dawson JB, Stephens WE (1975) Statistical classification of garnets from kimberlite and associated xenoliths. J Geol 83:589–607. doi:10.1086/628143

Deer WA, Howie RA, Zussman J (eds) (1992) An introduction to the rock-forming minerals (second edition). Pearson Prentice Hall, London

Enami M, Cong B, Yoshida T, Kawabe I (1995) A mechanism for Na incorporation in garnet: an example from garnet in orthogneiss from the Su-Lu terrane, eastern China. Am Mineral 80:475–482. doi:10.2138/am-1995-5-608

Gasparik T (1989) Transformation of enstatite-diopside-jadeite pyroxenes to garnet. Contrib to Mineral Petrol 102:389–405. doi:10.1007/BF00371083

Gasparik T (1990) Phase relations in the transition zone. J Geophys Res: Solid Earth 95:15751–15769. doi:10.1029/JB095iB10p15751

Green DH (1973) Experimental melting studies on a model upper mantle composition at high pressure under water-saturated and water-undersaturated conditions. Earth Planet Sci Lett 19:37–53. doi:10.1016/0012-821X(73)90176-3

Gregory HE (1916) Garnet deposits on the Navajo Reservation, Arizona and Utah. Eco Geol 11:223–230

Grütter HS, Gurney JJ, Menzies AH, Winter F (2004) An updated classification scheme for mantle-derived garnet, for use by diamond explorers. Lithos 77:841–857. doi:10.1016/j.lithos.2004.04.012

Helmstaedt H, Schulze DJ (1988) Eclogite-facies ultramafic xenoliths from Colorado Plateau diatreme breccias: comparison with eclogites in crustal environments, evaluation of the subduction hypothesis, and implications for eclogite xenoliths from diamondiferous kimberlites. In: Smith DJ (ed)

Eclogites and Eclogite-Facies Rocks. Developments in Petrology, vol 12. Elsevier, Amsterdam, pp 387–450

Irifune T, Hibberson WA, Ringwood AE (1989) In: Ross J (ed) Eclogite-garnetite transformation at high pressure and its bearing on the occurrence of garnet inclusions in diamond in Kimberlites and Related Rocks. Blackwell, Melbourne

Katayama I, Nakashima S, Yurimoto H (2006) Water content in natural eclogite and implication for water transport into the deep upper mantle. Lithos 86:245–259. doi:10.1016/j.lithos.2005.06.006

Leake BE, Woolley AR, Arps CES, Birch WD, Gilbert MC, Grice JD, Hawthorne FC, Kato A, Kisch HJ, Krivovichev VG, Linthout K, Laird J, Mandarino JA, Maresch WV, Nickel EH, Rock NMS, Schumacher JC, Smith DC, Stephenson NCN, Ungaretti L, Whittaker JW, Youzhi G (1997) Nomenclature of amphiboles: report of the subcommittee on amphiboles of the international mineralogical association, commission on new minerals and minerals names. Can Mineral 35:219–246

Libowitzky E, Rossman GR (1997) An IR absorption calibration for water in minerals. Am Mineral 82:1111–1115. doi:10.2138/am-1997-11-1208

Lu R, Keppler H (1997) Water solubility in pyrope to 100 kbar. Contrib to Mineral Petrol 129:35–42. doi:10.1007/s004100050321

Matsyuk SS, Langer K, Hösch A (1998) Hydroxyl defects in garnets from mantle xenoliths in kimberlites of the Siberian platform. Contrib to Mineral Petrol 132:163–179. doi:10.1007/s004100050414

Mookherjee M, Karato S (2010) Solubility of water in pyrope-rich garnet at high pressures and temperature. Geophys Res Lett 37. doi:10.1029/2009GL041289.

Moore RO, Gurney JJ (1985) Pyroxene solid solution in garnets included in diamond. Nature 318:553–555. doi:10.1029/2009GL041289

Ogasawara Y, Sakamaki K, Koga I (2012) Hydroxyl in garnets from Garnet Ridge, northern Arizona. AGU Fall Meeting 2012 abstract., pp V43A–2821

Ogasawara Y, Sakamaki K, Sato Y (2013) Water contents of garnets from the Garnet Ridge, northern Arizona: H_2O behavior underneath the Colorado Plateau. AGU Fall Meeting 2013 abstract., pp V23A–2754

O'Reilly SY, Griffin WL (2006) Imaging global chemical and thermal heterogeneity in the subcontinental lithospheric mantle with garnets and xenoliths: Geophysical implications. Tectonophysics 416:289–309. doi:10.1016/j.tecto.2005.11.014

Peacock SM (1993) The importance of blueschist → eclogite dehydration reactions in subducting oceanic crust. Geol Soc Am Bull 105:684–694. doi:10.1130/0016-7606(1993)105<0684:TIOBED>2.3.CO;2

Poli S, Schmidt MW (1995) H2O transport and release in subduction zones: experimental constraints on basaltic and andesitic systems. J Geophys Res 100:299–314. doi:10.1029/95JB01570

Ringwood AE (1967) The pyroxene-garnet transformation in the earth's mantle. Earth Planet Sci Lett 2:255–263. doi:10.1016/0012-821X(67)90138-0

Ringwood AE (1975) Composition and petrology of the Earth's mantle. McGraw-Hill, New York

Ringwood AE, Lovering JF (1970) Significance of pyroxene-ilmenite intergrowths among kimberlite xenoliths. Earth Planet Sci Lett 7:371–375. doi:10.1016/0012-821X(69)90052-1

Roden MF, Smith D, McDowell FW (1979) Age and extent of potassic volcanism on the Colorado Plateau. Earth Planet Sci Lett 43:279–284. doi:10.1016/0012-821X(79)90212-7

Sakamaki K, Ogasawara Y, Schertl HP (2014) OH and H_2O distributions in garnet of diamond-free and diamond-bearing garnet-clinopyroxene rocks from the Kokchetav Massif. AGU Fall Meeting 2014 abstract., pp V13B–4775

Sapienza GT, Scambelluri M, Braga R (2009) Dolomite-bearing orogenic garnet peridotites witness fluid-mediated carbon recycling in a mantle wedge (Ulten Zone, Eastern Alps, Italy). Contrib to Mineral Petrol 158:401–420. doi:10.1007/s00410-009-0389-2

Sato Y, Ogasawara Y (2013) Inclusion/lamella mineralogy and chemical characteristics of garnets from the Garnet Ridge in the Colorado Plateau, northern Arizona. AGU Fall Meeting 2013 abstract., pp V23A–2756

Sato Y, Koga I, Ogasawara Y (2014) Major element chemistry and inclusion/lamella mineralogy of garnets from the Garnet Ridge in the Colorado Plateau, northern Arizona. AGU Fall Meeting 2014 abstract., pp V13B–4777

Sautter V, Haggerty SE, Field S (1991) Ultradeep (>300 kilometers) ultramafic xenoliths: petrological evidence from the transition zone. Science 252:827–830. doi:10.1126/science.252.5007.827

Schulze DJ (2003) A classification scheme for mantle-derived garnets in kimberlite: a tool for investigating the mantle and exploring for diamonds. Lithos 71:195–213. doi:10.1016/S0024-4937(03)00113-0

Sakamaki *et al. Progress in Earth and Planetary Science* (2016) 3:20

Page 17 of 17

Schulze DJ, Davis DW, Helmstaedt H, Joy B (2015) Timing of the Cenozoic "Great Hydration" event beneath the Colorado Plateau: Th-Pb dating of monazite in Navajo volcanic field metamorphic eclogite xenoliths. Geology 43:727–730. doi:10.1130/G36932.1

Semken S (2003) Black rocks protruding up: the Navajo volcanic field. Geology of the Zuni Plateau: New Mexico. Geol Soc Guidebook 54:397–412

Shido F, Miyashiro A, Ewing M (1971) Crystallization of abyssal tholeiites. Contrib to Mineral Petrol 31:251–266. doi:10.1007/BF00374440

Smith D, Connelly JN, Manser K, Moser DE, Housh TB, McDowell FW, Mack LE (2004) Evolution of Navajo eclogites and hydration of the mantle wedge below the Colorado Plateau, southwestern United States. Geochem Geophys Geosyst 5:1–18. doi:10.1029/2003GC000675

Sobolev NV Jr, Lavrent'ev JG (1971) Isomorphic sodium admixture in garnets formed at high pressures. Contrib to Mineral Petrol 31:1–12. doi:10.1007/BF00373387

Song S, Zhang L, Liou JG, Niu Y (2005) Sodic amphibole exsolutions in garnet from garnet-peridotite, North Qaidam UHPM belt, NW China: implications for ultradeep-origin and hydroxyl defects in mantle garnets. Am Mineral 90:814–820. doi:10.2138/am.2005.1684

Sun SS, Nesbitt RW, Sharaskin AY (1979) Geochemical characteristics of mid-ocean ridge basalts. Earth Planet Sci Lett 44:119–138. doi:10.1016/0012-821X(79)90013-X

Switzer GS (1975) Composition of garnet xenocrysts from three kimberlite pipes in Arizona and New Mexico. Smithsonian Earth Sci 19:l–21

Usui T, Nakamura E, Kobayashi K, Maruyama S, Helmstaedt H (2003) Fate of the subducted Farallon plate inferred from eclogite xenoliths in the Colorado Plateau. Geology 31:589–592. doi:10.1130/0091-7613(2003)031<0589:FOTSFP>2.0.CO;2

Usui T, Nakamura E, Helmstaedt H (2006) Petrology and geochemistry of eclogite xenoliths from the Colorado Plateau: implications for the evolution of subducted oceanic crust. J Petrol 47:929–964. doi:10.1093/petrology/egi101

Usui T, Kobayashi K, Nakamura E, Helmstaedt H (2007) Trace element fractionation in deep subduction zones inferred from a lawsonite-eclogite xenolith from the Colorado Plateau. Chem Geol 239:336–351. doi:10.1016/j.chemgeo.2006.08.009

Van Roermund HLM, Drury MR, Barnhoorn A, De Ronde A (2001) Relict majoritic garnet microstructures from ultra-deep orogenic peridotites in western Norway. J Petrol 42:117–130. doi:10.1093/petrology/42.1.117

Vrijmoed JC, Austrheim H, John T, Hin RC, Corfu F, Davies GR (2013) Metasomatism in the ultrahigh-pressure Svartberget garnet-peridotite (western gneiss region, Norway): implications for the transport of crust-derived fluids within the mantle. J Petrol 54:1815–1848. doi:10.1093/petrology/egt032

Wang L, Essene EJ, Zhang Y (1999) Mineral inclusions in pyrope crystals from Garnet Ridge, Arizona, USA: implications for processes in the upper mantle. Contrib to Mineral Petrol 135:164–178. doi:10.1007/s004100050504

Wang L, Rouse RC, Essene EJ, Peacor DR (2000) Carmichaelite, a new hydroxyl-bearing titanate from Garnet Ridge, Arizona. Am Mineral 85:792–800. doi:10.2138/am-2000-5-620

Watson KD, Morton DM (1969) Eclogite inclusions in kimberlite pipes at Garnet Ridge, northeastern Arizona. Am Mineral 54:267–285

Withers AC, Wood BJ, Carroll MR (1998) The OH content of pyrope at high pressure. Chem Geol 147:161–171. doi:10.1016/S0009-2541(97)00179-4

Xia QK, Sheng YM, Yang XZ, Yu HM (2005) Heterogeneity of water in garnets from UHP eclogites, eastern Dabieshan, China. Chem Geol 224:237–246. doi:10.1016/j.chemgeo.2005.08.003